GA–A24333

THE 110 GHz MICROWAVE HEATING SYSTEM ON THE DIII–D TOKAMAK

by
J. LOHR, R.W. CALLIS, J.L. DOANE, R.A. ELLIS,
Y.A. GORELOV, K. KAJIWARA, D. PONCE, and R. PRATER

JULY 2003

DISCLAIMER

GA–A24333

THE 110 GHz MICROWAVE HEATING SYSTEM ON THE DIII–D TOKAMAK

by
J. LOHR, R.W. CALLIS, J.L. DOANE, R.A. ELLIS,*
Y.A. GORELOV, K. KAJIWARA,† D. PONCE, and R. PRATER

This is a preprint of a paper to be presented at the 15th Topical Conference on Radio Frequency Power in Plasmas, Moran,Wyoming, May 19–21, 2003 and to be published in the *Proceedings.*

*Princeton Plasma Physics Laboratory, Princeton, New Jersey.
†Oak Ridge Associated Universities, Oak Ridge, Tennessee.

Work supported by
the U.S. Department of Energy
under Contract Nos. DE-AC03-99ER54463, DE-AC02-76CH03073
and DE-AC05-76OR00033

GENERAL ATOMICS PROJECT 30033
JULY 2003

The 110 GHz Microwave Heating System on the DIII-D Tokamak

J. Lohr, R.W. Callis, J.L. Doane, R.A. Ellis,[a] Y.A. Gorelov, K. Kajiwara,[b] D. Ponce, and R. Prater

General Atomics, P.O. Box 85608, San Diego, California 92186-5608
[a]Princeton Plasma Physics Laboratory, Princeton, New Jersey.
[b]ORISE, Oak Ridge, Tennessee.

Abstract. Six 110 GHz gyrotrons in the 1 MW class are operational on DIII-D. Source power is >4.0 MW for pulse lengths ≤2.1 s and ~2.8 MW for 5.0 s. The rf beams can be steered poloidally across the tokamak upper half plane at off-perpendicular injection angles in the toroidal direction up to ±20°. Measured transmission line loss is about -1 dB for the longest line, which is 92 m long with 11 miter bends. Coupling efficiency into the waveguide is ~93% for the Gaussian rf beams. The transmission lines are evacuated and windowless except for the gyrotron output window and include flexible control of the elliptical polarization of the injected rf beam with remote controlled grooved mirrors in two of the miter bends on each line. The injected power can be modulated according to a predetermined program or controlled by the DIII-D plasma control system using real time feedback based on diagnostic signals obtained during the plasma pulse. Three gyrotrons have operated at 1.0 MW output power for 5.0 s. Peak central temperatures of the artificially grown diamond gyrotron output windows are <180°C at equilibrium.

INTRODUCTION

The last of the six 110 GHz gyrotrons in the DIII-D complex has successfully completed acceptance testing at full operational parameters of 80 kV and 40 A. The tube generated 1.0 MW rf output for 5.0 s. pulses. The completion of these tests marks the end of the present phase of system expansion and the beginning of a period of experiments in which additional operational flexibility will be added without increasing the number of gyrotrons installed. Three Gycom gyrotrons, with pulse lengths limited by heating of their boron nitride output windows, have been generating about 750 kW each for pulse lengths up to 2.1 s. and now three CPI gyrotrons equipped with low loss artificially grown diamond output windows have all been tested to 1.0 MW at 5.0 s pulse length.

All the Gycom gyrotrons were designed intentionally to spread the output rf beam over the 10 cm diameter of the BN windows to limit the peak power loading. Because the DIII-D transmission line is circular corrugated waveguide carrying the low loss $HE_{1,1}$ mode, a Gaussian rf beam had to be reformed using phase correcting mirrors effectively to excite the $HE_{1,1}$ mode. Although this could be done so that a good quality Gaussian waist was formed at the waveguide input, the efficiency of this recovery process was never much higher than about 87% and sometimes was lower.

With the advent of artificially grown diamond gyrotron windows capable of handling the full power Gaussian beam without damage, it became possible to couple to waveguide simply using a single ellipsoidal mirror with ≈93% overall efficiency.

HARDWARE

The six gyrotrons are connected to three dual articulating launchers, which can direct the rf beams poloidally over the tokamak upper half plane and ±20° toroidally to the angles for peak current drive efficiency in both the co- and counter-current drive directions. Following damage to one launcher sustained due to rf-driven arcing, these launchers are now being monitored by video cameras and Langmuir probes in addition to the normal temperature measurements on the mirrors using resistance temperature devices (RTDs). The launchers have also been made more robust thermally by replacement of the aluminum launcher waveguides with stainless steel guides having silver plating on the inner bores. Photographs of one of the launchers on the bench and installed in the tokamak are shown in Fig. 1. The video view of the launcher from the tokamak flange seen in D_α light during a plasma discharge is shown in Fig. 2.

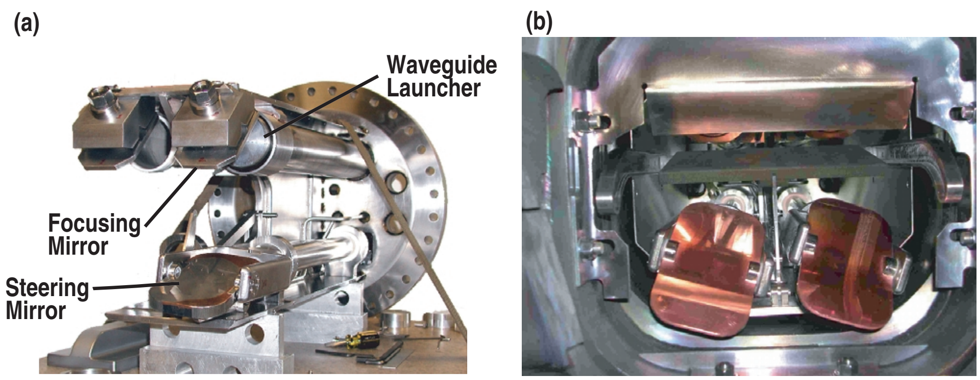

FIGURE 1. View of one of the articulating launchers on the bench. The mirrors can rotate to scan toroidally and tilt for the poloidal scan, although the two motions are not orthogonal.

One consistent challenge for the DIII-D installation has been the estimation of the power injected into the plasma from each of the launchers. Although calorimetric measurements of the power loading of the gyrotron components and the transmission line are made on every shot, and these can be related to the injected power, the accuracy of this procedure when compared with diagnostic measurements of plasma electron heating has been poor. A prototype design for a power monitor to be located near the tokamak is shown in Fig. 3. This vacuum compatible device simply consists of a small gap in the transmission line surrounded by a cylindrical volume into which a small fraction of the transmitted power is radiated. The cylinder has an annular ring of TiO_2 at the location of the waveguide gap, which absorbs most of the leakage rf power. A pair of RTD sensors differentially measures the temperatures of the cylinder wall at the

TiO_2 strip and the end plate, giving a time dependent signal the peak value of which is proportional to the integral of the rf power during the pulse. In preliminary tests, a 250 ms pulse at ≈500 kW gave a 2°C peak temperature difference between the RTDs.

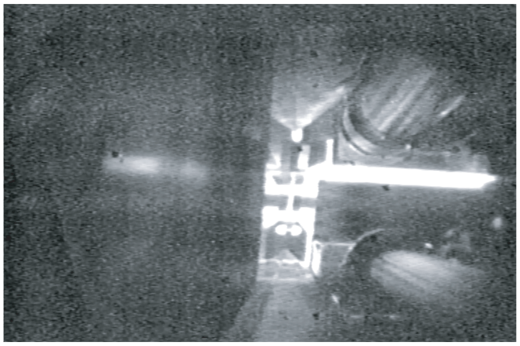

FIGURE 2. Video view of a launcher assembly seen in plasma light. The lower tube is the mirror actuator and the upper is the launcher waveguide. The second launcher is on the right border.

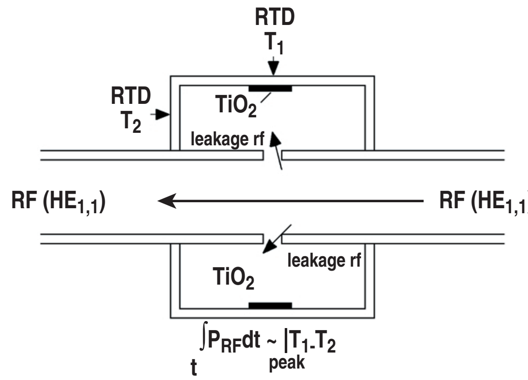

FIGURE 3. Schematic of a prototype rf power monitor. The vacuum compatible unit measures heating from leakage rf power.

GYROTRON CONDITIONING

In general, gyrotrons are delivered to DIII-D from the manufacturers following a period of testing at the factory. In the case of Communications and Power Industries (CPI) production, the tubes are factory tested at about 550 kW for 10 s pulses and for short pulses several ms in duration at 1.0 MW rf output. The available test stand at CPI is limited to 25 A for long pulse operation, limiting the maximum performance testing.

Recently a gyrotron was delivered to DIII-D after major replacement of sections of the collector but without any factory testing. The *ab initio* conditioning performed at DIII-D required about 2.5 months of around the clock operation to achieve full parameter operation at 1.0 MW rf output. In Fig. 4, the progression of pulse length extension at different gyrotron electron beam currents is plotted as a function of calendar day. Initial operation was at low beam currents, but the current was rapidly increased to 25 A, after which pulse extension to 1.0 s required about 4 weeks. After an additional week, 2.5 s pulses were achieved, but an increase in beam current to 30 A restarted the process, with about a week required to return to 1.0 s pulses at the higher current. The current was increased to the full value, 40 A, whereupon several days were required to achieve 2.0 s and after about a week 5.0 s pulses had been fired.

The conditioning process was begun at each step by reducing the magnetic field from the upper main coil until rf generation was lost, establishing the low field operating limit. By only changing the upper main coil, the field geometry near the gun is barely affected. The magnetic field was increased by ≈2% so that operation was reliable, albeit at the expense of output power. Once full length pulses were obtained, the magnetic field was carefully decreased until the peak in the output power was observed. Conditioning was interrupted twice for repairs to the high voltage power supply.

The output power was measured calorimetrically using several algorithms. A typical subset of calorimetry traces is presented in Fig. 5. Analysis of these traces was performed both by using digital oscilloscopes and by an automatic system. Fluctuating baselines were problematic for both methods. The generated rf power estimates rely on measured window loss, on the relationship between cavity rf power loading and generated power, on the efficiency at peak tuning and on the rf power actually absorbed in the dummy loads. The power/heating relationships were measured in the CPI test stand, where a very simple power collection setup routinely achieves total power accountability >97% overall. In the DIII-D system, coupling to waveguide, rf beam conditioning and focusing, a relatively long line to the dummy loads, several miter bends and a complex shared cooling water system combine to decrease the accuracy of the calorimetric measurements. Unmonitored rf power of at least 100 kW has been measured using an infrared camera viewing the transmission line components when the rf beam is directed into the dummy loads. If this power is taken into account, the dummy load measurements still have a 10% discrepancy compared with the cavity measurements. In Fig. 6, the results of the automatic analysis are presented.

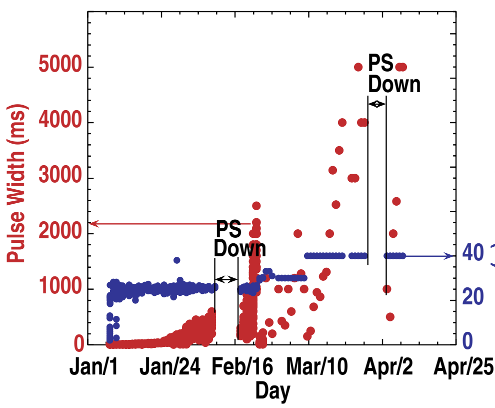

FIGURE 4. Summary of the progression of *ab initio* gyrotron conditioning. The gyrotron was conditioned to 1.0 MW, 5.0 s operation at 80 kV and 40 A in about 2.5 months of around the clock operation.

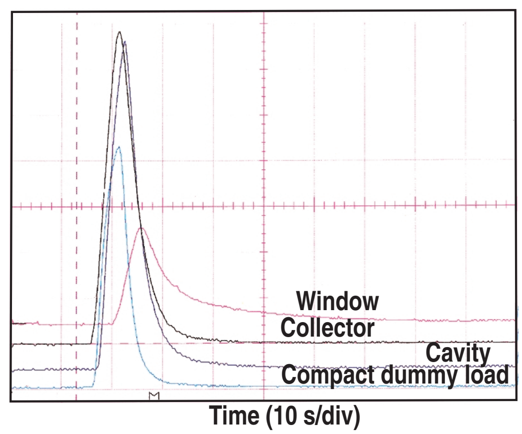

FIGURE 5. Calorimetric measurements of rf heating of the diamond output window, the collector, cavity and compact dummy load. The vertical scales are arbitrary.

The figure plots measurements of the generated rf power inferred from several calorimetric data sets taken separately at full gyrotron parameters, 80 kV, 40 A and peak tuning of the magnetic fields as a function of pulse length. The data fall into bands at constant power, indicating systematic errors in the measurement using each data set. The highest power estimate comes from subtracting the collector power from the input electrical power and assuming an efficiency of 34%. This method typically gives ≈1.3 MW for the generated rf power estimate. Possibly the most accurate power measurement is obtained from the cooling for the gyrotron cavity. This loading was accurately measured at CPI and should be 2.32% of the generated power. Using this measurement, the automatic system indicates peak generated power of 1 MW at 5.0 s pulses. The power absorbed in the gyrotron output window is only about 0.2%, which gives calorimetric temperature differences of less than a degree C for most operations. The window cooling water also cools the window support and exit waveguide. This makes it difficult to infer the window transmitted power to sufficient accuracy for plasma experiments. In most cases the automatic calorimetry system underestimates the output power but when the same data are analyzed manually with a digital oscilloscope transmitted powers in agreement with the cavity measurements are obtained.

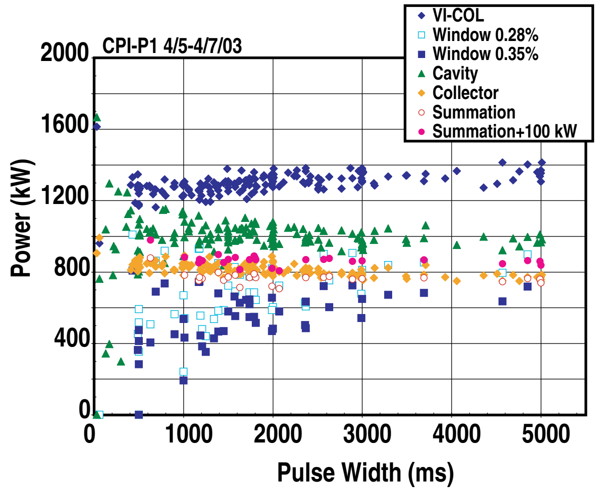

FIGURE 6. Summary of calorimetric data as a function of pulse length. The data for each of the cooling circuits are multiplied by predetermined scale factors to give a measurement of the generated rf power. The data reveal systematic patterns of disagreement at the ±20% indicating that additional corrections must be applied.

SUMMARY

The DIII-D 110 GHz ECH system has been expanded to a six gyrotron system with flexible launch capability. The system generates about 5 MW and about 4 MW reaches the tokamak for experiments.

ACKNOWLEDGMENT

Work supported by the U.S. Department of Energy under Contracts DE-AC03-99ER54463, DE-AC02-76CH03073, and DE-AC05-76OR00033.